Surface Functions during Mitosis in Rat Basophilic Leukemia Cells

J. M. OLIVER, JC. SEAGRAVE, J. R. PFEIFFER, M. L. FEIBIG, and G. G. DEANIN
Department of Pathology, University of New Mexico School of Medicine, Albuquerque, New Mexico 87131

ABSTRACT   At the entry into mitosis, cells abruptly lose membrane activities such as phago-cytosis, pinocytosis, and capping. The present studies test if mitotic cells also resist functional responses to cell surface ligand–receptor interactions. The IgE receptors of RBL-2H3 rat basophilic leukemia cells were labeled with anti-dinitrophenol IgE (anti–DNP-IgE) and then cross-linked with multivalent ligands (DNP–bovine serum albumin [BSA]; DNP–B-phycoery-thrin; DNP-BSA-gold). IgE–receptor cross-linking modulates cell surface organization and function and releases serotonin and other mediators of allergic and asthmatic reactions from interphase cells (Pfeiffer, J. R., JC. Seagrave, B. H. Davis, G. G. Deanin, and J. M. Oliver, 1985, J. Cell Biol., 101:2145–2155). It was found that anti–DNP-IgE-receptor complexes are preserved on the cell surface throughout mitosis; they continue to bind DNP–proteins, and the resulting antigen–IgE–receptor complexes can redistribute to coated pits on the cell surface. Further-more, there is no loss of [^{3}H]serotonin through mitosis. Nevertheless, antigen-stimulated [^{3}H]-serotonin release is strongly impaired in mitotic-enriched as compared with mixed interphase or G_1-enriched cell populations. In addition, antigen binding transforms the surface of inter-phase cells from a microvillous to a plicated topography and stimulates the uptake of fluorescein isothiocyanate–conjugated dextran by fluid pinocytosis. Mitotic cells maintain a microvillous surface topography after antigen treatment, and fluid pinocytosis virtually ceases from prometaphase to telophase. Phorbol myristate acetate, a tumor promoter that activates protein kinase C, restores surface ruffling activity to mitotic cells. Thus, the mitosis-specific freezing of membrane and secretory responses is most likely due to the failure of transmem-brane signaling.

We have postulated that mitosis may represent a period when animal cells are specifically and reversibly insulated from environmental regulation. This hypothesis is based on the arrest in macrophages and other cells of a range of dynamic membrane functions (phagocytosis, pinocytosis, capping) at the onset of mitosis and their resumption at the entry of cells into G_1 (22). The hypothesis predicts that cells should be incapable of response to hormones, growth factors, and im-mune effectors during mitosis. Consistent with this, Radley and Hodgson (26) have demonstrated that mitotic cells of the parotid and submaxillary glands are specifically resistant to isoprenaline-induced degranulation in vivo, Howard and Sheppard (14) have summarized and expanded the extensive evidence for low levels of cyclic AMP and correspondingly low activities of adenylate cyclase during mitosis, and Preston et al. (25) have demonstrated that the adhesion and spreading

of Cloudman M3 melanoma cells induced by melanocyte-stimulating hormone is inhibited during mitosis. Recently Hesketh et al. (13) reported that the IgE-mediated release of histamine from rat basophil leukemia cells is reduced during mitosis.

We report here further studies of the responses of mitotic RBL-2H3 cells to IgE–receptor cross-linking. RBL-2H3 cells were selected because (a) they can be synchronized (7) without use of anti-microtubule drugs that may disturb membrane functions, (b) their biochemical (1, 2, 19) and morphological (24) responses to cross-linking of cell surface IgE–receptor complexes with multivalent antigens have been well charac-terized, and (c) their high density of IgE receptors (15) coupled with the recent development of new fluorescent antigens (10, 24) enables ready analysis of antigen–receptor binding, clus-

tering, and internalization. Preliminary accounts of these experiments have appeared in abstract form (23).

MATERIALS AND METHODS

Cells and Reagents: These are described in the companion paper (24).

Synchronization: For mitotic collection, RBL-2H3 cells were grown as monolayers in 100 ml Dulbecco's modified Eagle's medium with 15% fetal calf serum (DME–FCS)[1] on 1,000-ml glass Blake bottles (Blake Industries, Inc., Scotch Plains, NJ). They were synchronized by release from double thymidine block (2.5 mM TdR 2 × 8-h incubations, separated by 12 h in DME–FCS plus 10 μM deoxycytidine) and manual (20 s) mitotic shake-off by a modification of the procedure of Buell et al. (7). Alternatively, they were synchronized by release from single hydroxyurea block (5 mM hydroxyurea; 10 h) and 3-s mechanical mitotic shake-off by a modification of the procedure of Tobey et al. (30). Either two or four Blake bottles of cells were used for each experiment. Both thymidine and hydroxyurea block cells at the G_1/S boundary.

In general the peak of mitosis occurred between 6 and 8 h after release of cells from thymidine or hydroxyurea block. To obtain mitotic populations without resorting to treatments that disrupt microtubules (anti-microtubule drugs or drastic cooling), cells were harvested by mitotic shake-off and 3-min centrifugation every 20 min beyond 5 h of release. After each shake at room temperature, 50 ml of fresh 37°C DME–FCS was added to the cell monolayers, and the Blake bottles were returned immediately to the 37°C incubator. Meanwhile, the shake-off medium was centrifuged for 3 min in a Sorvall GSA centrifuge (Beckman Instruments, Inc., Fullerton, CA), the resulting cell pellets were resuspended in 0.5 ml Hanks' medium (3) containing 0.05% bovine serum albumin (Hanks'–BSA), and portions were incubated for 30 s with the DNA-specific vital stain Hoechst 33342 (100 μg/ml). The percentage of mitotic cells was determined by counting mitotic figures in a Zeiss fluorescence microscope (Carl Zeiss, Inc., Thornwood, NY). The early washes removed poorly adherent interphase cells. When degranulation assays followed, these washes served the additional purpose of removing excess [^{3}H]serotonin and anti-dinitrophenol IgE (anti–DNP-IgE).

Mitotic collection was begun when the shake-off reached 60% mitotic cells. Cells shaken off in 50 ml DME–FCS were concentrated into 1 ml Hanks'–BSA and held at room temperature until sufficient numbers were collected (at least 3 × 10^6 cells; usually three shakes at 10-min intervals). After mitotic collection the Blake bottles were returned to the incubator with 50 ml fresh DME–FCS for another 2 h. Early G_1 populations, which are poorly adherent to the surface, were then collected by another series of three shakes followed by 30 min in the CO_2 incubator (to encourage progression of lagging mitotic cells into G_1). Finally, mixed interphase cells were collected by scraping the cells that remained after the G_1 harvest.

[^{3}H]Serotonin Release: [^{3}H]Serotonin (2 μCi/ml) and anti–DNP-IgE (3 μg/ml) were added to the culture medium at 1–2 h after the removal of thymidine or hydroxyurea. The cells were undisturbed for 2–4 h. They were then washed extensively with DME–FCS and harvested as described above. The compositions of the pooled mitotic, G_1, and mixed interphase harvests were confirmed by Hoechst staining, and 0.2-ml portions of cells were dispensed immediately into triplicate tubes containing 0.02 ml of 10 mM HEPES buffer 7.4 alone or HEPES with DNP-proteins (usually 1 μg/ml). The amount of [^{3}H]serotonin released in 15 min was determined as described (24).

Fluorescence and Electron Microscopy: Cells were labeled with dinitrophenol-conjugated B-phycoerythrin (DNP-PhE), fluorescein isothiocyanate–conjugated dextran (fluorescein–dextran), and rhodamine–phalloidin as described (24). To identify mitotics, the nuclei of fixed cells were also labeled by incubation for an additional 10 min with 2 μg/ml Hoechst 33342, before rinsing, mounting, and observation by epillumination in a Zeiss photomicroscope III. Cells were processed for transmission and scanning electron microscopy as described (24).

Flow Cytometry: The efficiency of synchronization was followed by flow cytometry. Cells harvested by scraping at hourly intervals after removal of thymidine or hydroxyurea were fixed in 70% ethanol and their DNA labeled with propidium iodide. The amount of DNA per cell was measured using

---

[1] *Abbreviations used in this paper:* anti–DNP-IgE, anti-dinitrophenol IgE; DME–FCS, Dulbecco's modified Eagle's medium with 15% fetal calf serum; DNP–BSA, dinitrophenol-conjugated bovine serum albumin; DNP–PhE, dinitrophenol-conjugated B-phycoerythrin; fluorescein–dextran, fluorescein isothiocyanate–conjugated dextran; Hanks'–BSA, Hanks' medium with 0.05% bovine serum albumin; PMA, phorbol myristate acetate.

Sorter II in the National Flow Cytometry Resource at Los Alamos National Laboratories (29). Data were collected as percentage of cells in G_1, S, and $G_2 + M$. The percentage of mitotic (M) cells was determined by fluorescence microscopy of cells labeled for 10 min at 37°C with 2 μg/ml Hoechst 33342.

RESULTS

Synchronization

About 60% of thymidine-blocked cells are in early S phase as judged by flow cytometric analyses of their DNA content after labeling with propidium iodide. Upon removal of thymidine they progress in a fairly synchronous manner to G_2 and mitosis ($G_2 + M$) and finally to G_1. The distribution of cells through these various phases with time after release of thymidine block is shown in Fig. 1A. The presence of anti–DNP-IgE had no effect on the progression of synchronized cells through the cell cycle.

In cells released from thymidine block, mitotic shake-off yields populations that are 50–60% mitotic over a period of ~1 h (Fig. 1B). Cell kinetics and mitotic yields of hydroxyurea-treated cells are closely similar to those of thymidine-blocked cells.

Mitotic cells can be assigned to one of five mitotic stages based on the distribution of the fluorescent dye Hoechst 33342: prophase, prometaphase, metaphase, anaphase, and telophase. The criteria for these assignments were developed previously (5), and most stages are illustrated in the micrographs that follow. Briefly, chromosomes are condensed and intercoiled and the nuclear envelope disassembles during
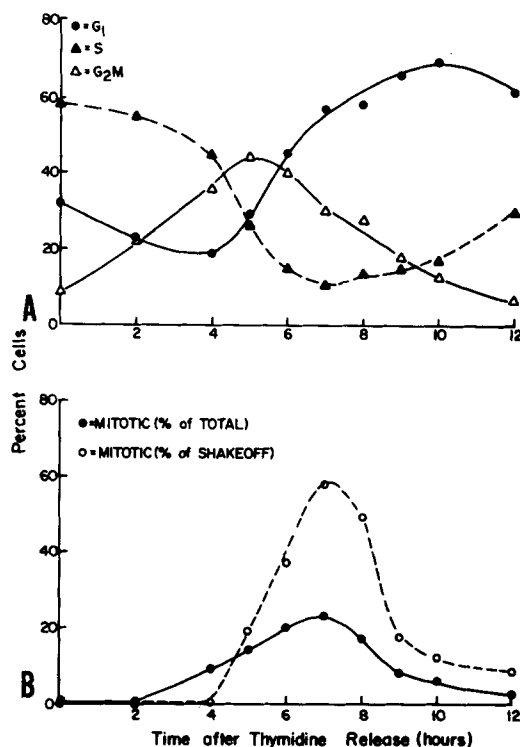

FIGURE 1 The synchronization of RBL-2H3 cells. In A, cells were harvested by scraping at hourly intervals after removal of medium containing 2.5 mM thymidine and its replacement with medium containing 10 μm deoxycytidine. Their distribution between the S, $G_2 + M$, and G_1 phases of the cell cycle was determined by flow cytometry after labeling with propidium iodide. In B, the proportion of mitotic cells was determined by fluorescence microscopy after collecting the entire population by scraping or after collecting the mitotic-enriched cells by shake-off.

prophase; chromosomes become elongated, separated, and partially aligned during prometaphase; chromosomes assume a highly ordered, equatorial arrangement (the metaphase plate) at metaphase; at anaphase sister chromatids are separated and the cleavage furrow appears; and telophase cells show partly decondensed, widely separated chromosomes and a deep cleavage furrow. In synchronized RBL-2H3 ~60% of the mitotic harvest is metaphase cells, and the remaining cells are distributed between prometaphase, anaphase, and telophase. Cells in prophase are not detached by mitotic shake-off. A high proportion of the contaminating interphase cells are G_1 pairs that have not yet reattached to the Blake bottles.

Characteristic Properties of Mitotic RBL-2H3 Cells

DNP-PHE BINDING: Fig. 2 shows that DNP-PhE binds at 4°C to both mitotic and interphase cells. Furthermore, microspectrophotometric measurements of DNP-PhE binding at 4°C revealed a small (~10%) but consistent increase in the relative fluorescence intensity of the mitotics as compared with cells judged to be in S or G_2 based on their large size and the high relative intensity of nuclear fluorescence due to Hoechst 33342. As expected, early G_1 cells, recognized by their small size and low relative intensity of Hoechst 33342 labeling, bound approximately half as much DNP-PhE as did the mitotics.

[^{3}H]SEROTONIN CONTENT: The [^{3}H]serotonin content per cell is highest in mitotic-enriched populations. In four experiments, mixed interphase populations contained ~80% as much [^{3}H]serotonin per cell as the mitotics, and G_1-enriched populations contained ~60% as much [^{3}H]serotonin per cell as the mitotic populations (Table I).

Properties of Antigen-stimulated Mitotic Cells

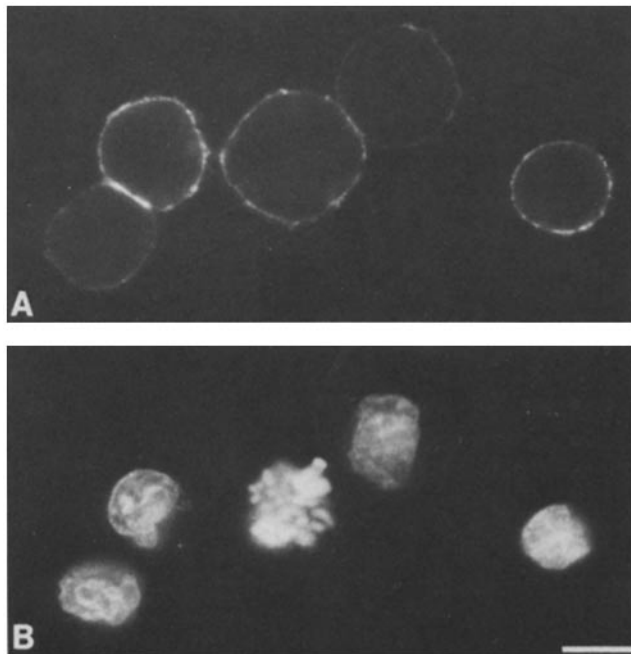[^{3}H]SEROTONIN RELEASE: In four experiments, bind-

FIGURE 2 Binding of DNP-PhE to RBL-2H3 cells. Anti-DNP-IgE–treated RBL-2H3 cells were incubated for 10 min at 4°C with 1 μg/ml DNP-PhE (A), then fixed and their DNA labeled with Hoechst 33342 (B). Fluorescent antigen is associated with both the interphase and mitotic (prometaphase) cells. Bar, 10 μm.

TABLE I.   [^{3}H]Serotonin Content Is Normal but IgE-mediated Release of [^{3}H]Serotonin Is Impaired during Mitosis

Cell population	Total [^{3}H]serotonin content (% of mitotic enriched population)	Percentage of total [^{3}H]serotonin released by DNP-protein
Mitotic enriched (average 47% M)	100	6.63 ± 2.25
G_1 enriched (average 70% G_1 pairs; 10% M)	59.3 ± 4.16	13.58 ± 3.23
Mixed interphase (average 5% M; 5% G_1 pairs)	80.8 ± 8.0	12.28 ± 3.42

Results are the average ± SD of duplicate or triplicate determinations in four separate experiments. Within each experiment mitotic (M), G_1, and mixed interphase cells were harvested sequentially from the same Blake bottles of anti-DNP-IgE–primed cells. Total serotonin content was determined by Triton extraction of anti-DNP-IgE–primed cell populations. Stimulated serotonin release was measured after 15-min incubation of cells with 1 μg/ml DNP-BSA or DNP-B-phycoerythrin. Note that the mitotic-enriched populations were initially >60% mitotic. The lower final mitotic index of the pooled cells (average 47% M; range 35–60%) reflects the progression of some cells to G_1 after harvest.

TABLE II.   [^{3}H]Serotonin Release Is Specifically Impaired during Mitosis

Cell population	Fractional degranulation	P
Mitotic enriched vs. G_1	0.46 ± 0.13	<0.005
Mitotic enriched vs. mixed interphase	0.52 ± 0.12	<0.005
G_1 enriched vs. mixed interphase	0.94 ± 0.39	NS

The [^{3}H]serotonin released by DNP-BSA from anti-DNP-IgE–primed mitotic-enriched (47%) cells was expressed as a fraction of [^{3}H]serotonin released from G_1-enriched (70% G_1 pairs, 10% M) and mixed interphase (5% G_1 pairs, 5% M) cells harvested from the same Blake bottles. Results are the mean ± SE of these values for fractional release obtained in four separate experiments. Student's t test was used for the statistical analysis. NS, not significant.

ing of DNP-BSA and DNP-PhE to anti-DNP-IgE-receptor complexes stimulated the release of ~13% of the total [^{3}H]-serotonin content of G_1-enriched and mixed interphase cells in 15 min (Table I). Cell populations that were ~50% mitotic released only 7% of their total [^{3}H]serotonin content in response to IgE–receptor cross-linking. These values are corrected for spontaneous [^{3}H]serotonin release that remained approximately the same (between 4 and 6% [^{3}H]serotonin release in 15 min) in mitotic-enriched, G_1-enriched, and mixed interphase cell populations.

In Table II the stimulated release of [^{3}H]serotonin from mitotic cells is expressed as the fraction of stimulated [^{3}H]-serotonin release from G_1 and mixed interphase cells harvested from the same culture bottles. The data from four experiments were averaged and analyzed statistically using Student's t test. Cell populations that are ~50% mitotic release ~50% as much [^{3}H]serotonin in response to IgE–receptor cross-linking as do the interphase cell populations. These differences are highly significant ($P \leq 0.005$). There is no significant difference between G_1 and mixed interphase cells in stimulated [^{3}H]serotonin release.

SURFACE TOPOGRAPHY: In the preceding paper the topography of unstimulated and antigen-stimulated RBL-2H3 cells was observed by scanning electron microscopy and by examination of rhodamine-phalloidin–labeled cells in the fluorescence microscope. It was shown that anti-DNP-IgE–primed RBL-2H3 cells have a characteristically microvillous

cell surface in the absence of antigen. Dinitrophenol–conjugated bovine serum albumin (DNP–BSA) treatment transforms the surface of interphase cells to a highly plicated topography.

The same analysis was performed here using mitotic-enriched populations. In the absence of antigen, both mitotic and interphase cells have a microvillous surface topography (Fig. 3A). Interphase cells are all plicated after incubation for
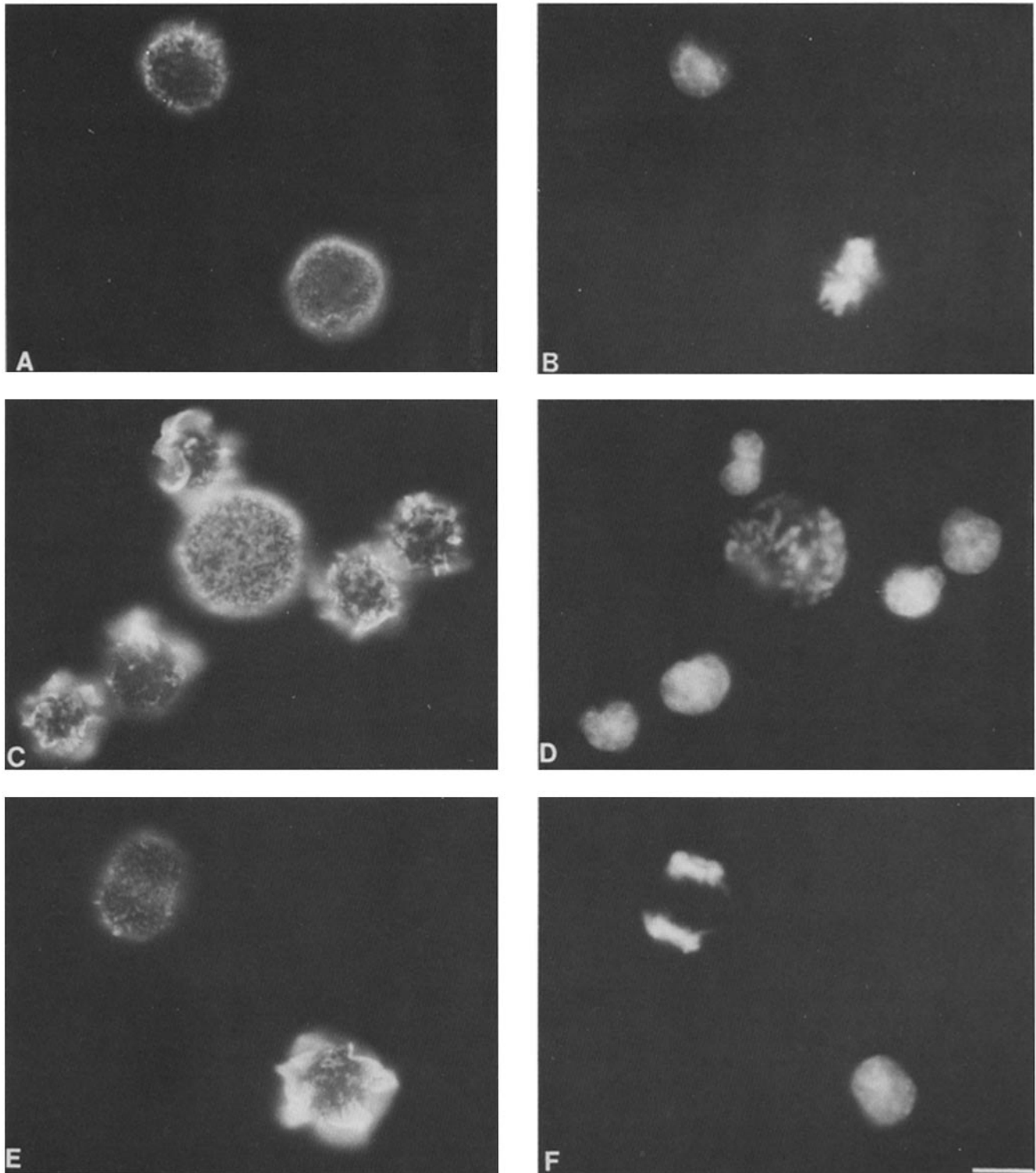

FIGURE 3 Surface topography of mitotic cells: fluorescence microscopy. Suspensions of RBL-2H3 cells were incubated with or without DNP–BSA at 37°C for 10 min, then fixed and labeled with rhodamine–phalloidin and with Hoechst 33342. The cells were photographed to emphasize the topography of the upper cell surface. A 40× planapochromatic objective with partially closed diaphragm was used to minimize out-of-focus fluorescence at the cell periphery. In the absence of antigen, both interphase and mitotic (metaphase) cells have a microvillous cell surface (A and B). All the antigen-treated interphase cells show a plicated surface topography (C–F). The cells in prometaphase (C and D) and anaphase (E and F) are persistently microvillous. Bar, 10 μm.
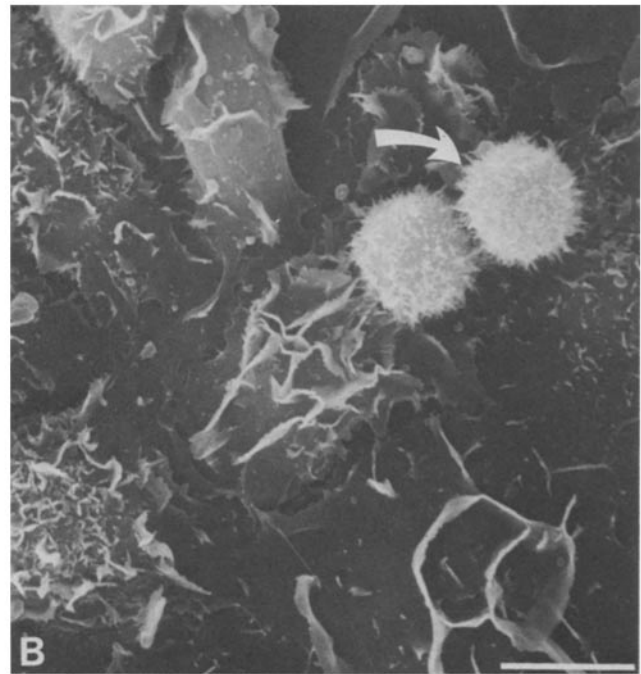
FIGURE 4 Surface topography of mitotic cells: Scanning electron microscopy. Mitotic-enriched cell monolayers were incubated for 15 min in 1 μg/ml DNP-BSA, rinsed gently to minimize displacement of loosely adherent mitotic cells, and processed for scanning electron microscopy. Most cells show a plicated surface topography. The arrow in A points to a microvillous cell that is in early anaphase. The arrow in B points to a microvillous cell pair that is most likely in late anaphase. Other cells that are rounded and maintain a microvillous cell surface (cells on either side of the anaphase cell in A, for example) are also probably mitotic but this cannot be proven by scanning electron microscopy. Bars, 10 μm.

10 min with antigen (Fig. 3, C and E). However, the prometaphase cell in Fig. 4C and the anaphase cell in Fig. 3E maintain a persistently microvillous surface topography. Antigen-induced membrane plications were also observed by scanning electron microscopy on essentially all interphase cells, but never on cells judged from their shapes to be in anaphase or telophase (Fig. 4). Cells at earlier mitotic stages could not be identified with certainty by scanning electron microscopy.

Rhodamine-phalloidin–labeled cell populations were scored for their microvillous or plicated surface topography as a function of the mitotic cycle. Fig. 5A shows that cells in prophase and some prometaphase cells develop surface plications in response to antigen binding. Essentially all cells in metaphase and anaphase maintain a microvillous surface topography in the presence of antigen.

FLUID PINOCYTOSIS: Cross-linking of anti–DNP-IgE-receptor complexes by DNP-BSA on interphase cells stimulates the uptake of fluorescein–dextran by fluid pinocytosis (24). Mitotic cells between prometaphase and telophase internalize very little fluorescein–dextran in the presence or absence of DNP-BSA. This selective impairment of fluid uptake is illustrated in Fig. 6.

The results of population analyses of fluorescein-dextran-labeled cells are plotted as a bar graph in Fig. 7A. Fluid pinocytosis is reduced during prometaphase and is arrested in metaphase and anaphase.

Dynamic Properties of Antigen–IgE–Receptor Complexes during Mitosis

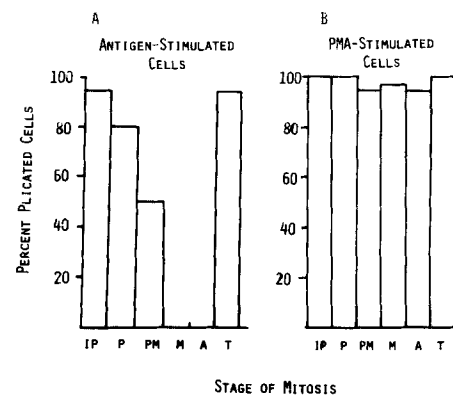INTERNALIZATION OF LIGAND–IGE–RECEPTOR COMPLEXES: DNP–proteins bound to IgE–receptor com-

FIGURE 5 Surface transformation induced by antigen binding and PMA. IgE-primed cells were incubated for 10 min at 37°C in Hanks'–BSA containing 1 μg/ml DMP-BSA (A) on 10 nM PMA (B). They were fixed and labeled with rhodamine–phalloidin to outline membrane topography and with Hoechst 33342 to identify mitotic stages. Mitotic and interphase cells were scored in the fluorescence microscope for the presence of surface plications. At least 100 cells were observed for each mitotic stage. IP, interphase; P/PM, prophase/prometaphase; M, metaphase; A, anaphase; T, telophase.

plexes on interphase cells are rapidly redistributed to cytoplasmic vesicles that are visible by fluorescence microscopy of DNP-PhE–labeled cells and by transmission electron microscopy of DNP-BSA-gold–labeled cells (24). To determine if mitotics also internalize antigen, anti–DNP-IgE–primed, mitotic-enriched RBL-2H3 cells were incubated for 10 min at 37°C with DNP-PhE, followed by 2 min with the monovalent competing ligand, DNP-lysine, to displace most of the surface fluorescence. Intracellular DNP-PhE-IgE–receptor
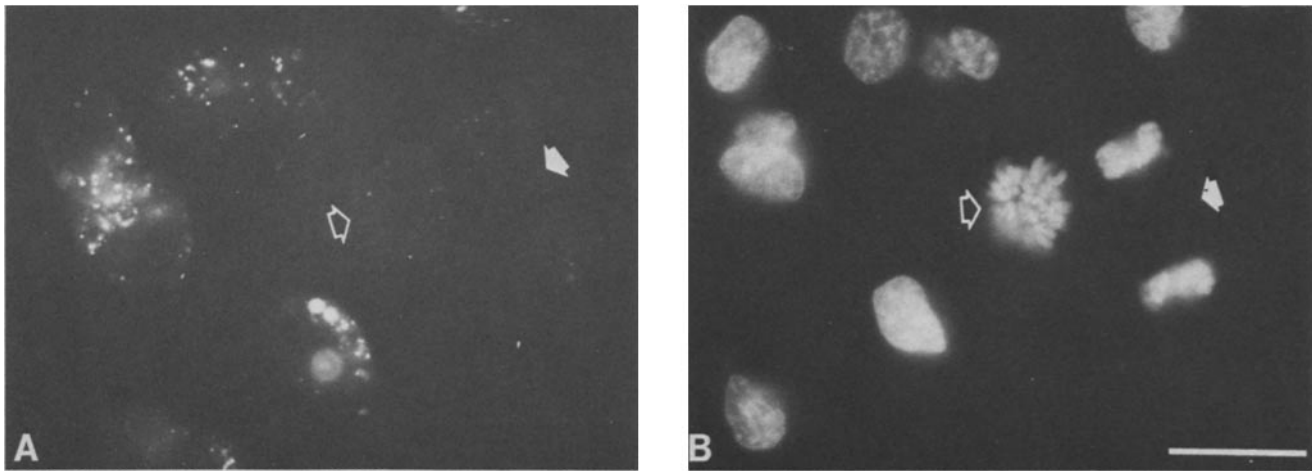
FIGURE 6 Fluid pinocytosis by interphase and mitotic cells. Anti-DNP-IgE-treated RBL-2H3 cells were incubated for 10 min at 37°C with Hanks'-BSA containing 1 μg/ml DNP-BSA and 20 mg/ml fluorescein-dextran (A). They were rinsed, fixed, and their DNA labeled with Hoechst 33342 (B). The interphase cells have all internalized fluorescein-dextran. There is no fluorescein-dextran uptake during metaphase (open arrows) and anaphase (closed arrows). Bar, 10 μm.
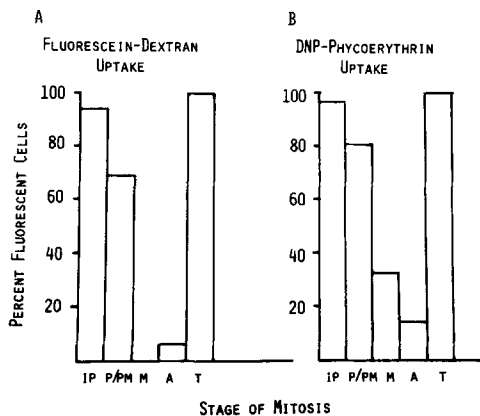

FIGURE 7 Fluorescein-dextran uptake and DNP-PhE uptake as a function of the mitotic cycle. IgE-primed cells were incubated for 10 min at 37°C in Hanks'-BSA containing 1 μg/ml DNP-BSA plus 20 mg/ml fluorescein-dextran (A) or with 1 μg/ml DNP-PhE (B). They were then fixed, and their DNA was labeled with Hoechst 33342. Mitotic and interphase cells were scored in the fluorescence microscope for the presence of intracellular vesicles containing fluorescein (A) or DNP-PhE (B). At least 100 cells were observed for each mitotic stage.

complexes were observed by fluorescence microscopy. DNP-PhE is internalized by most prometaphase cells (Fig. 8A) and by many metaphase cells (Fig. 8C). Anaphase cells internalize little or no antigen (Fig.8E), but internalization resumes by telophase (Fig.8G).

The results of population analyses of DNP-PhE-labeled cells are plotted in Fig. 7B. Almost all cells in prophase, prometaphase, and telophase can support the uptake of DNP-PhE-IgE-receptor complexes. However, only ~35% of metaphase cells internalize antigen, and only 15% of anaphase cells show uptake of DNP-PhE.

Redistribution of Antigen-IgE-Receptor Complexes to Coated Pits

DNP-BSA-gold particles are redistributed into coated pits on the cell surface of interphase RBL-2H3 cells before internalization. In the preceding paper (24) we showed that ~25%

of surface-associated particles are in coated pits on interphase cells incubated for 2, 5, and 10 min with DNP-BSA-gold, whereas the proportion of intracellular gold particles increases steadily with time. These data indicate that a continuous process of binding, redistribution, and internalization of DNP-BSA-gold occurs during interphase.

Cells in mitosis also accumulate surface-bound gold particles in coated pits. Thus the anaphase cell in Fig. 9 was incubated for 10 min at 37°C with DNP-BSA-gold. 44 gold particles are bound and 37 (84%) of these particles are on the cell surface. The small number of intracellular particles is consistent with the reduction in antigen uptake established by fluorescence microscopy of anaphase cell. 12 (27%) of the surface-associated particles are in coated pits. The inset to Fig. 9 shows a portion of a metaphase (M) cell and a neighboring interphase (IP) cell from the same DNP-BSA-gold-labeled sample. The metaphase cell had 31 gold particles bound over its entire surface, of which 14 (45%) were in coated pits. The segment of the cell shown here has one coated pit that contains eight gold particles. Only one intracellular particle is visible. The interphase cell also has gold associated with a coated pit at the cell surface. In addition, numerous gold-containing cytoplasmic vacuoles are present. In a sample of 10 mitotic cells (six in prometa- or metaphase; four in ana- or telophase) that were similarly labeled for 10 min with DNP-protein-gold, no more than 50% of the total gold particles were even in the cytoplasm, and between 27% (the anaphase cell in Fig. 9) and 68% (a telophase cell) of surface-bound particles were in coated pits.

PMA Induces Surface Transformation in Mitotic Cells

The tumor promoter phorbol myristate acetate (PMA) was shown previously to transform the interphase cell surface from a microvillous to a plicated topography (24). Fig. 10 establishes that PMA can also transform the surface of mitotic cells. This transformation occurs on essentially every mitotic cell (Fig. 5B).

DISCUSSION

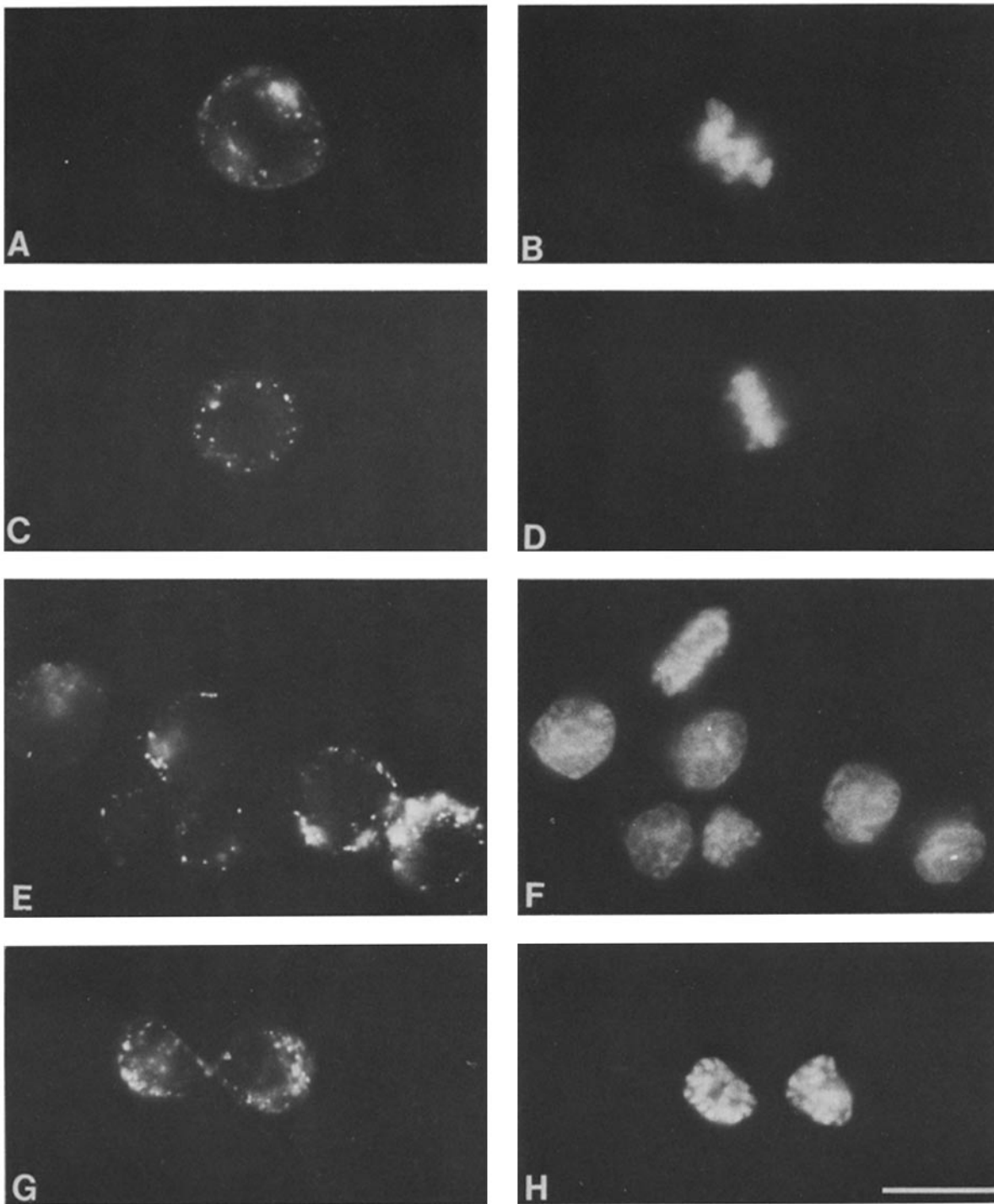We set out to test the hypothesis that mitotic cells are specif-

FIGURE 8 The internalization of antigen during mitosis. Anti-DNP-IgE-treated cells were incubated for 10 min with 1 μg/ml DNP-PhE, followed by 2 min with 10 μM DNP-lysine. They were fixed and their nuclei labeled with Hoechst 33342. DNP-PhE is internalized by the cells in interphase (E and F), prometaphase (A and B), metaphase (C and D), and telophase (G and H). The cell in early anaphase (E and F) shows no intracellular fluorescence. Bar, 10 μm.

ically and reversibly resistant to activation by hormones, growth factors, and immune effectors that bind to membrane receptors on target cells. The RBL-2H3 cell line was selected for analysis for several reasons.

First, the biochemical and morphological responses leading to the antigen-stimulated release of mediators ([³H]serotonin, histamine) from the secretory granules of interphase RBL-2H3 cells are fairly well defined. Briefly, antigen binding cross-links IgE–receptor complexes and leads, most likely via acti-

vation of a GTP-binding protein, to the increased hydrolysis of inositol phospholipids by phosphatidylinositol bisphosphate phosphodiesterase. This hydrolysis yields diacylglycerol that stimulates protein kinase C as well as inositol trisphosphate that mobilizes Ca^{2+} (1, 2, 9, 21). Antigen binding also causes an initial decrease followed by a marked increase in membrane-associated filamentous actin (24). These biochemical responses are accompanied by the transformation of membrane topography from microvillous to plicated, by an
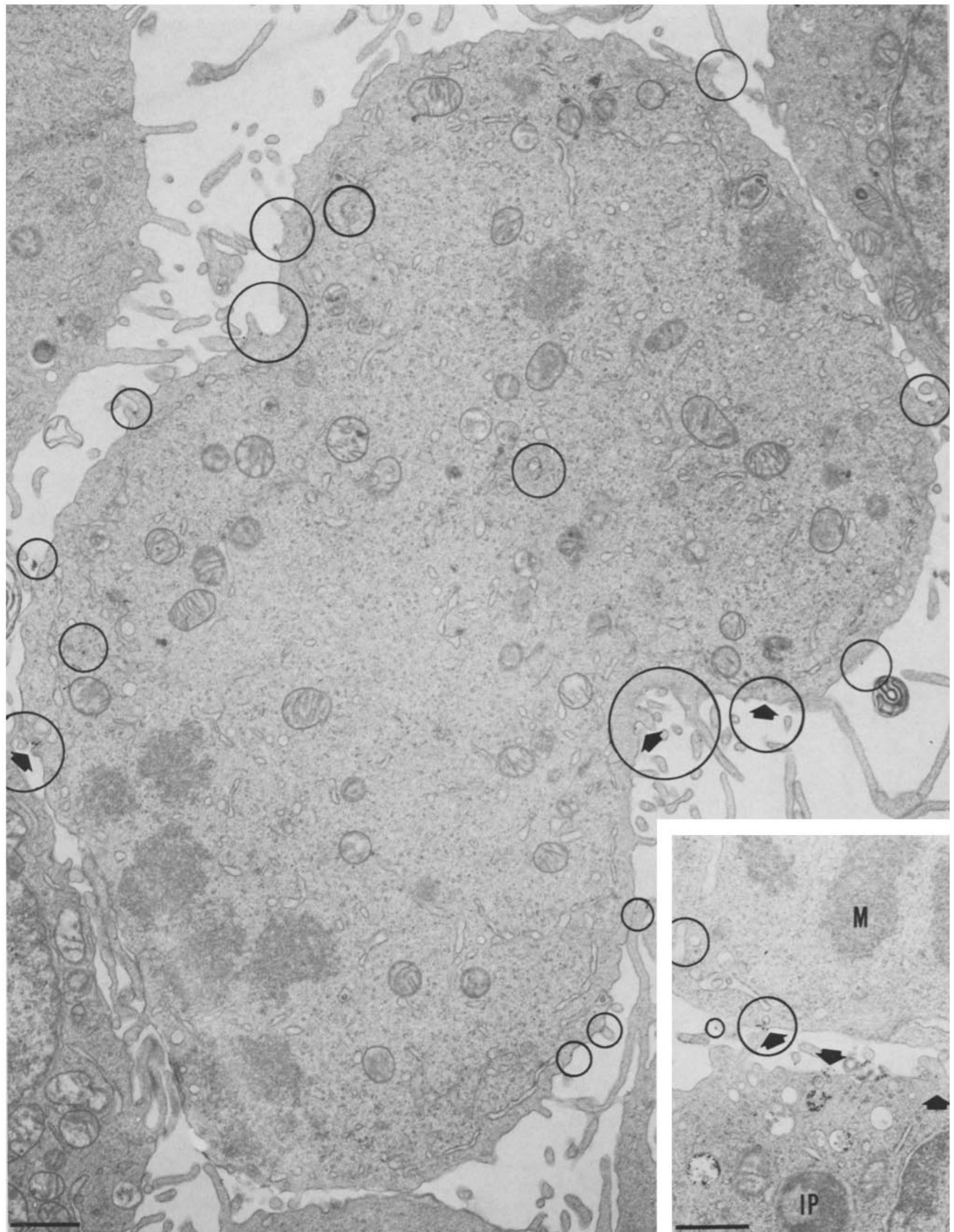
FIGURE 9   The distribution of gold–DNP–BSA during mitosis. Mitotic-enriched anti–DNP–IgE–primed cells were incubated for 10 min with DNP–BSA (1 µg/ml). In the anaphase cell, surface-bound gold particles (circles) are associated with unspecialized membrane and with the membranes of coated pits (arrows). There are very few intracellular gold particles. Similarly the segment of a metaphase cell (inset) shows gold accumulated in a coated pit at the cell surface but only one intracellular particle. The inset also shows a segment of an interphase cell (IP) that has internalized a large number of gold particles. Bars, 1 µm.
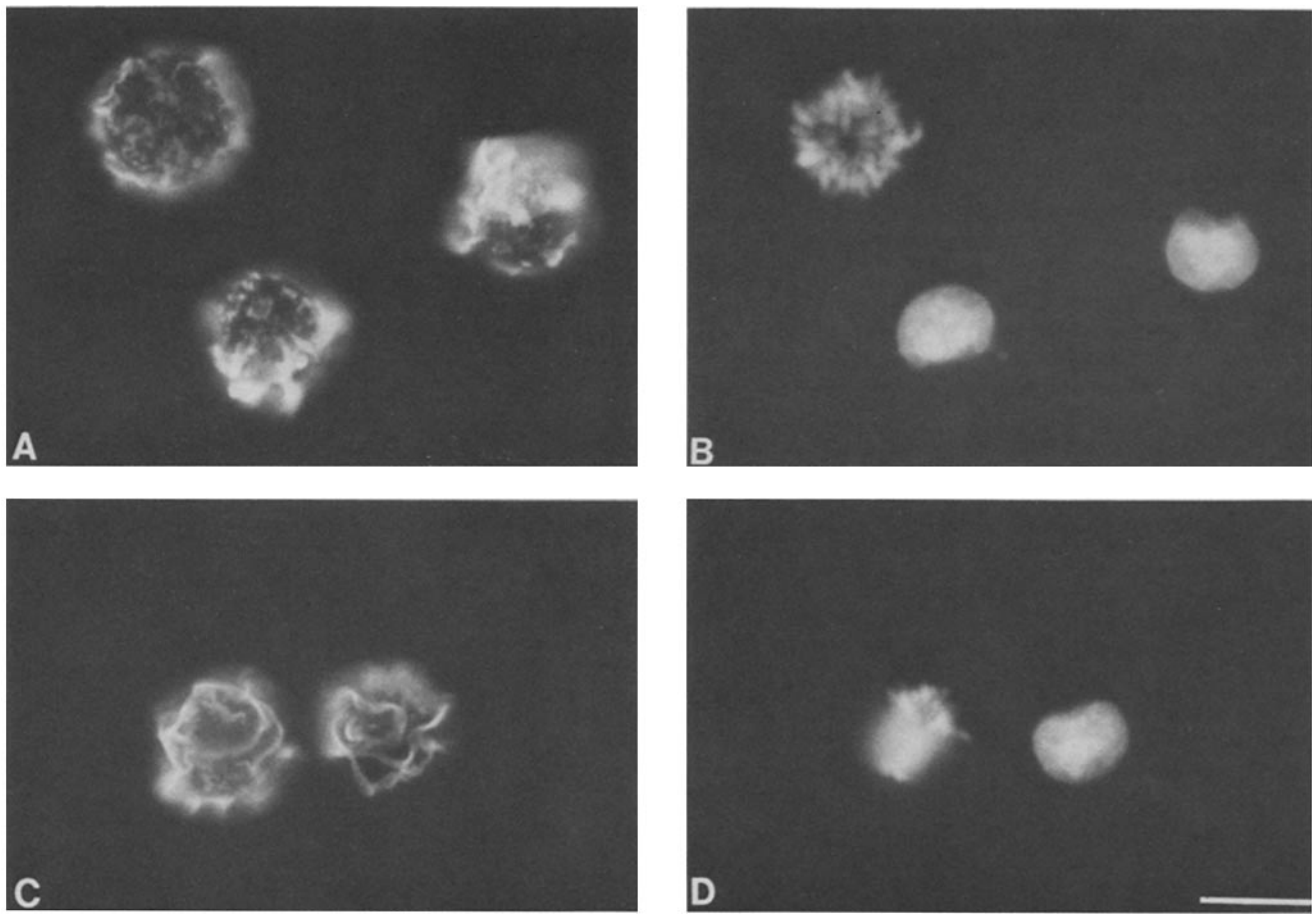
FIGURE 10 Surface transformation induced by PMA. Cells were incubated with 10 nM PMA, then labeled with rhodamine-phalloidin (A and C) and Hoechst 33342 (B and D) and photographed to display the topography of the upper cell surface as described in the legend to Fig. 4. The interphase cells, as well as the metaphase cell in A and B and the prometaphase cell in C and D, are all extensively plicated. Bar, 10 μm.

increased rate of fluid pinocytosis, and by enhanced cell spreading (24).

Second, each interphase cell has more than 10^5 IgE receptors (16) and the mobility in the membrane and internalization of IgE–receptor complexes can be followed by use of fluorescent (8, 18, 24), radiolabeled (11, 16), and gold-conjugated (24) antigens, respectively.

Third, cell populations that are ~60% mitotic can be obtained by release from G_1/S blocking agents (thymidine and hydroxyurea) and subsequent mitotic shake-off. Higher yields of mitotic cells are possible if nocodazole or colchicine are used to prevent their progression beyond mitosis (13). However in our hands nocodazole and colchicine (0.1–10 μM; 1–3 h) inhibit [³H]serotonin release from interphase RBL-2H3 cells by 20–50%. A similar inhibition of degranulation follows microtubule disassembly in primary mast cells and basophils (12, 27). In addition we have reported that anti-microtubule drugs have different effects on the shape and membrane properties of mitotic and interphase cells (4). Thus, a function that seems unaltered by these drugs in interphase cells may be altered during mitosis. For these reasons, we chose to use imperfectly synchronized cells rather than infer normal mitotic properties from the responses of drug-treated cells.

We found that DNP–PhE binds to anti–DNP-IgE-receptor complexes on mitotic cells, and that the intensity of fluorescence per mitotic cell is somewhat higher than the average

fluorescence intensity per interphase basophil. This indicates that IgE receptors (and IgE–receptor complexes) are preserved throughout mitosis. Similarly, Isersky et al. (15) reported that IgE–receptor density on RBL-2H3 cells is high during mitosis and is maximal during G_1. Meyer et al. (20) confirmed a high density of IgE receptors in G_2 + M cells although they found low receptor density on G_1 cells. We also found that mitotic-enriched populations have higher concentrations of [³H]serotonin than either mixed interphase or G_1-enriched cells harvested from the same culture bottles. These data indicate that there is no loss of [³H]serotonin to the medium during the progression of unstimulated cells from S and G_2 through mitosis. There is of course a reduction in [³H]serotonin content per cell in G_1 as a result of the division of granules between daughter cells at cytokinesis.

Even though IgE–receptor complexes and intracellular mediators are preserved throughout mitosis, anti–DNP-IgE–treated RBL-2H3 cells release very little [³H]serotonin when incubated with DNP–proteins during mitosis. However cells that bound IgE during S and G_2 can release [³H]serotonin in response to antigen after progression to G_1. Similarly, Hesketh et al. (13) have reported that nocodazole-arrested mitotic RBL cells fail to show antigen-IgE–dependent histamine release. Thus, antigen-stimulated mediator release is specifically and reversibly inhibited during mitosis.

Several other membrane responses to IgE–receptor cross-

linking are also impaired during mitosis in RBL-2H3 cells. In particular, interphase cells show a characteristic transformation of cell surface topography from a microvillous to a plicated appearance after antigen binding to IgE–receptor complexes (24). This surface response is arrested during prometaphase and is not restored until telophase. In addition, IgE–receptor cross-linking causes an immediate 2-3-fold stimulation of fluid pinocytosis by interphase cells. Like surface transformation, this response is substantially decreased in prophase/prometaphase, and fluid pinocytosis is not observed by fluorescence microscopy in metaphase and anaphase cells. The internalization of antigen per se is also reduced, although to a smaller extent than antigen-stimulated surface transformation and fluorescein–dextran uptake. Thus, the uptake of DNP–PhE into cytoplasmic fluorescent vesicles persists into metaphase and is strongly inhibited only in anaphase. Even anaphase cells can redistribute DNP–BSA–gold particles into coated pits, indicating that antigen–IgE–receptors retain at least some capacity for lateral movement through mitosis.

These results provide strong support for our starting hypothesis that signals produced by the interaction of specific ligand with surface receptors on target cells are either not generated or not recognized during mitosis.

How are mitotic cells isolated from environmental control? Warren and colleagues (13) reported that antigen binding to populations of nocodazole-arrested mitotic cells increase cytoplasmic free Ca^{2+} levels to ~50% of interphase levels. From this, they concluded that transmembrane signal generation is preserved during mitosis. They proposed that the impairment of cellular functions, including IgE-mediated release of histamine from RBL-2H3 cells, results from a generalized absence of membrane fusion and budding reactions during mitosis (13, 31). This hypothesis successfully predicts the impairment of both endocytic and exocytic processes during mitosis, as demonstrated in basophils and many other cell types (4–6, 13, 26, 28, 31, 32). However, it cannot easily explain why the transformation of RBL-2H3 cell surface topography from a microvillous to a plicated organization is inhibited during mitosis. Our previous demonstration that melanocyte-stimulating hormone fails to induce adhesion and spreading of mitotic melanoma cells (25) is also difficult to explain solely on the basis of the absence of membrane fusion and budding reactions.

Our data indicate that the failure of antigen-mediated cell responses during mitosis is indeed the result of impaired transmembrane signaling. The evidence for this comes from pharmacological studies. As noted, antigen binding normally stimulates the hydrolysis of phosphatidylinositol bisphosphate, generating diacylglycerol that activates protein kinase C and inositol trisphosphate that stimulates Ca^{2+} mobilization. In the companion paper (24) we established that the membrane responses to IgE–receptor cross-linking are mimicked by PMA, the tumor promoter that directly stimulates protein kinase C activity. Antigen-dependent mediator release is mimicked by the ionophore A23187 plus Ca^{2+}, that directly mobilizes Ca^{2+}. We report here that PMA can transform the surface of mitotic cells from a microvillous to a plicated topography. This indicates that protein kinase C is present during mitosis, and both mitotic and interphase cells can support membrane and cytoskeletal responses to protein kinase C–mediated phosphorylation reactions. We conclude that antigen-stimulated surface transformation is inhibited

during mitosis due to a defect in the transduction pathway that leads from antigen binding to protein kinase C activation.

Ligand-stimulated Ca^{2+} mobilization is considered to be controlled by the same transduction pathway as ligand-stimulated protein kinase C activity (21). It is thus surprising that Warren and colleagues (13) found only a partial inhibition during mitosis of ligand-stimulated Ca^{2+} mobilization in Quin-2-labeled, nocodazole-arrested mitotic RBL-2H3 cells. An improved shake-off method to isolate 90% pure (or better) mitotic RBL-2H3 cells is being refined in our laboratory. We predict that A23187 plus Ca^{2+} will stimulate [^{3}H]serotonin release from these mitotic populations. We intend to reexamine antigen-stimulated Ca^{2+} uptake and free Ca^{2+} levels in these cells.

The improved mitotic populations will also simplify biochemical analyses of the signaling defect. We predict that changes in antigen binding affinity or in the kinetics of antigen-induced IgE–receptor cross-linking are responsible for the failure of signal transduction during mitosis. However the absence from the membrane or inactivation during mitosis of the GTP-binding protein (transducer) or phosphatidylinositol bisphosphate phosphodiesterase would also prevent transmembrane signaling in mitotic cells.

REFERENCES

1. Beaven, M. A., J. Rogers, J. P. Moore, T. R. Hesketh, G. A. Smith, and J. C. Metcalfe. 1984. The mechanism of the calcium signal and correlation with histamine release in 2H3 cells. *J. Biol. Chem.* 259:7129–7136.
2. Beaven, M. A., J. P. Moore, G. A. Smith, T. R. Hesketh, and J. C. Metcalfe. 1984. The calcium signal and phosphatidylinositol breakdown in 2H3 cells. *J. Biol. Chem.* 259:7137–7142.
3. Becker, E. L. 1972. The relationship of the chemotactic behavior of the complement-derived factors, C3A, C5A and C567, and a bacterial chemotactic factor to their ability to activate the proesterase of rabbit polymorphonuclear leukocytes. *J. Exp. Med.* 135:376–387.
4. Berlin, R. D., J. R. Pfeiffer, R. J. Walter, and J. M. Oliver. 1980. Surface functions in dividing macrophages. *In* Mononuclear Phagocytes. Functional Aspects. Part I. R. Van Furth, editor. Martinus Nijhoff, The Hague. 705–732.
5. Berlin, R. D., J. M. Oliver, and R. J. Walter. 1978. Surface functions during mitosis. I. Phagocytosis, pinocytosis and mobility of surface-bound Con A. *Cell.* 15:327–341.
6. Berlin, R. D., and J. M. Oliver. 1980. Surface functions during mitosis. II. Quantitation of pinocytosis and kinetic characterization of fluorescence technique. *J. Cell Biol.* 85:660–671.
7. Buell, D. N., B. J. Fowlkes, H. Metzger, and C. Isersky. 1976. Cell cycle and morphological changes during growth and differentiation of a rat basophilic leukemia cell line. *Cancer Res.* 36:3131–3137.
8. Carson, D. E., and H. Metzger. 1974. Interaction of IgE with rat basophilic leukemia cells. IV. Antibody-induced redistribution of IgE receptors. *J. Immunol.* 113:1271–1277.
9. Cockcroft, S., and B. D. Gamperts. 1985. Role of guanine nucleotide binding protein in the activation of polyphosphatidylinositide phosphodiesterase. *Nature (Lond.).* 214:534–536.
10. Deanin, G. G., B. H. Davis, R. P. Haugland, JC. Seagrave, C. C. Stewart, J. Steinkamp, and J. M. Oliver. 1984. The DNP-phycobiliproteins, a new family of fluorescent ligands to study IgE-mediated degranulation in rat basophilic leukemia cells. *J. Cell Biol.* 99(4, Pt. 2):331a. (Abstr.)
11. Furuichi, K., J. Rivera, and C. Isersky. 1984. The fate of IgE bound to rat basophilic leukemia cells. III. Relationship between antigen-induced endocytosis and serotonin release. *J. Immunol.* 133:1513–1520.
12. Gillespie, E., and L. M. Lichtenstein. 1972. Histamine release from human leukocytes: studies with deuterium oxide, colchicine and cytochalasin B. *J. Clin. Invest.* 51:2941–2947.
13. Hesketh, T. R., M. A. Beaven, J. Rogers, B. Burke, and G. B. Warren. 1984. Stimulated release of histamine by a rat mast cell line is inhibited during mitosis. *J. Cell Biol.* 98:2250–2254.
14. Howard, R. F., and J. R. Sheppard. 1981. Cell cycle changes in the adenylate cyclase of C6 glioma cells. *J. Cell Biol.* 90:169–175.
15. Isersky, C., H. Metzger, and D. N. Buell. 1975. Cell cycle-associated changes in receptors

for IgE during growth and differentiation of a rat basophil leukemia cell line. *J. Exp. Med.* 141:1147-1162.

16. Isersky, C., J. Rivera, D. M. Segal, and T. Triche. 1983. The fate of IgE bound to rat basophilic cells. II. Endocytosis of IgE oligomers and effect on receptor turnover. *J. Immunol.* 131:388-396.

17. Jesaitis, A. J., J. R. Naemura, L. A. Sklar, C. G. Cochrane, and R. G. Painter. 1984. Rapid modulation of N-formyl chemotactic peptide receptors on the surface of human granulocytes: formation of high affinity ligand-receptor complexes in transient association with cell cytoskeleton. *J. Cell Biol.* 98:1378-1387.

18. Menon, A. K., D. Holowka, and B. Baird. 1984. Small oligomers of immunoglobulin E (IgE) cause large-scale clustering of IgE receptors on the surface of rat basophilic leukemia cells. *J. Cell Biol.* 98:577-583.

19. Metzger, H., and T. Ishizaka. 1982. Transmembrane signaling by receptor aggregation: the mast cell receptor for IgE as a case study. *Fed. Proc.* 42:7-34.

20. Meyer, C., L. M. Wahl, B. M. Stadler, and R. P. Siraganian. 1983. Cell cycle associated changes in histamine release from rat basophilic leukemia cells separate by counterflow centrifugal elutriation. *J. Immunol.* 121:911-914.

21. Nishizuka, Y. 1984. The role of protein kinase C in cell surface signal transduction and tumor promotion. *Nature (Lond.).* 308:693-698.

22. Oliver, J. M., and R. D. Berlin. 1982. Mechanisms that regulate the structural and functional architecture of cell surfaces. *Int. Rev. Cytol.* 74:55-94.

23. Oliver, J. M., J. R. Pfeiffer, JC. Seagrave, and G. G. Deanin. 1984a. The failure of transmembrane signalling during mitosis: IgE-mediated degranulation is reversibly arrested in mitotic rat basophilic leukemia cells. *J. Cell Biol.* 99(4, Pt. 2):449a. (Abstr.)

24. Pfeiffer, J. R., JC. Seagrave, B. H. Davis, G. G. Deanin, and J. M. Oliver. 1985. Membrane and cytoskeletal changes associated with IgE-mediated serotonin release in rat basophilic leukemia cells. *J. Cell Biol.* 101:2145-2155.

25. Preston, S. F., R. D. Berlin, and J. M. Oliver. 1982. Immediate effects of MSH on melanoma cells in culture. *J. Cell Biol.* 95(2, Pt. 2):195a. (Abstr.)

26. Radley, J. M., and G. S. Hodgson. 1971. Effect of isoprenaline on cells in different phases of the mitotic cycle. *Exp. Cell Res.* 69:148-160.

27. Ranadive, N. S. 1978. Histamine release from mast cells and basophils. *In* Inflammation, Immunity and Hypersensitivity. H. Z. Movat, editor. Harper and Row. 375-409.

28. Sager, P. R., P. A. Brown, and R. D. Berlin. 1984. Analysis of transferrin recycling in mitotic and interphase HeLa cells by quantitative fluorescence microscopy. *Cell.* 39:275-282.

29. Steinkamp, J. 1984. Flow cytometry. *Rev. of Sci. Instrum.* 55:1375-1400.

30. Tobey, R. A., E. C. Anderson, and D. F. Petersen. 1967. Properties of mitotic cells prepared by mechanically shaking monolayer cultures of Chinese hamster cells. *J. Cell. Physiol.* 70:63-68.

31. Warren, G., C. Featherstone, G. Griffiths, and B. Burke. 1983. Newly synthesized G protein of vesicular stomatitis virus is not transported to the cell surface during mitosis. *J. Cell Biol.* 97:1623-1628.

32. Zeligs, J. D., and S. H. Wollman. 1979. Mitosis in rat thyroid epithelial cells *in vivo.* I. Ultrastructural changes in cytoplasmic organelles during the mitotic cycle. *J. Ultrastruct. Res.* 66:58-77.